

## Adapting elastic wavefield extrapolation to laterally varying HTI media

Richard A. Bale and Gary F. Margrave

### ABSTRACT

Elastic wavefield extrapolators have been derived for HTI media which vary only in the depth direction, based upon eigensolutions to the Kelvin-Christoffel equation. Here, we extend elastic wavefield extrapolation to laterally heterogeneous media, using PSPI and NSPS type pseudodifferential operators, as has previously been done for scalar wavefield extrapolation. As in that case, we observe that forward extrapolation with PSPI and reverse extrapolation with NSPS (or vice versa) better recovers the input, than does use of either algorithm in both directions. Thus, NSPS and PSPI appear to be adjoint operators when applied in opposing directions of extrapolation.

Elastic wavefield extrapolation in HTI media can be formulated in two alternative ways. The first is based upon extrapolation of a continuous displacement-stress vector by eigen-decomposition into wave-modes, propagation through each homogeneous layer, and recomposition at a new depth. The second is based upon extrapolation of the wave-modes within homogeneous layers, and application of “interface-propagators” to cross layer interfaces. For laterally invariant media, the two approaches give identical results, with the interface-propagator method having a performance advantage. In the laterally heterogeneous case, the two approaches can give different results. To be specific, the latter method suffers polarization errors when formulated for the same efficiency gain as is possible in the homogeneous case. Nevertheless, for media with gradual continuous changes of anisotropic symmetry axis, this more efficient approach gives acceptable results.

### INTRODUCTION

In a companion paper (Bale and Margrave, 2003), we discuss the design of wavefield extrapolators for elastic, HTI (transversely isotropic, with a horizontal symmetry axis) media. That paper assumes that the medium varies only in the vertical direction. Here we investigate the extension to more realistic media which have lateral variation of properties. The problem of *acoustic* extrapolation in laterally varying media has been the subject of much previous research within the CREWES and POTSI consortia (e.g. Margrave and Ferguson, 1998, 1999, 2000; Ferguson and Margrave, 2002; Grossman et al., 2002a). The conceptual framework which has been developed is to represent the ideal extrapolation operator as a pseudodifferential operator in which the phase shift applied depends on both  $x$  and  $k_x$  simultaneously.

There are two elementary, alternative ways this can be done, depending on whether the operator integral transforms the wavefield from the Fourier domain back to the spatial domain, referred to as PSPI (Gazdag and Sguazzero, 1984), or from the spatial domain forward to the Fourier domain, referred to as NSPS (Margrave and Ferguson, 1999). These correspond to the standard and adjoint forms of a

pseudodifferential operator respectively. In either case, practical implementation of the operator is achieved by a windowed Fourier transform so that FFT codes can be used. A new method known as adaptive Gabor phase-shift (AGPS), which aims to optimize this windowing based on the spatial variation of the model, is currently being investigated (Grossman et al., 2002a, 2002b).

In this paper, our goal is to show how the PSPI and NSPS approaches apply to *elastic* wavefield extrapolation, and to discuss some specific issues which arise in this context. In the next section we briefly review the theory for extrapolation in laterally homogeneous media, explained at more length in Bale and Margrave (2003), before proceeding to look at PSPI and NSPS formulations of that theory. We consider an alternative formulation using the “interface-propagator” matrix, which offers efficiency advantages, but proves to have limitations due to implicit inconsistencies between decomposition and recombination steps. The subsequent section illustrates the extrapolation operators with numerical examples for laterally discontinuous media. Finally we put forward some conclusions.

### THEORY

As described in Bale and Margrave (2003), for wave propagation in a 2-D laterally homogeneous HTI medium with horizontal slowness  $s_x = k_x/\omega$ , the elastic extrapolation operator is

$$\mathbf{b}(s_x, z_{n+1}, \omega) = \mathbf{D}_n e^{i\omega\Lambda_n(z_{n+1}-z_n)} \mathbf{D}_n^{-1} \mathbf{b}(s_x, z_n, \omega), \quad (1a)$$

where  $\mathbf{b}$  is a vector containing displacement and the vertical components of stress, properties which are continuous across a horizontal plane, given by

$$\mathbf{b} = \begin{pmatrix} \mathbf{u} \\ \boldsymbol{\tau} \end{pmatrix}, \text{ for } \boldsymbol{\tau} = -\frac{1}{i\omega} (\sigma_{13} \quad \sigma_{23} \quad \sigma_{33})^T. \quad (1b)$$

The 6-by-3 matrix  $\mathbf{D}_n$  contains the eigenvectors,  $\mathbf{b}_n^{(M)}$ , for each mode  $M \in \{P, S1, S2\}$ , which are one-way solutions (down-going for forward extrapolation) to the wave equation  $\partial\mathbf{b}/\partial z = i\omega\mathbf{A}\mathbf{b}$  in layer  $n$ .  $\mathbf{A}$  is the fundamental elasticity matrix (e.g. Ting, 1996). The subscript  $n$  refers to the layer below the  $n^{\text{th}}$  interface, with layers chosen such that vertical variation of the medium may be neglected. Layer  $n$  lies between  $z_n$  and  $z_{n+1}$ . The diagonal matrix  $\Lambda_n = \text{diag}(q_n^P \quad q_n^{S1} \quad q_n^{S2})$  contains the vertical slownesses for each mode in layer  $n$ . Both  $\mathbf{D}_n$  and  $\Lambda_n$  depend on  $s_x$ , but not on  $\omega$ , nor, in this case, on  $x$ .

In words, equation (1) states the following: decompose the displacement-stress wavefield at depth  $z_n$  into the three eigenstates for layer  $n$  which are the elastic modes; propagate each mode using the vertical slowness for that mode; recombine the modes at the new depth  $z_{n+1}$ . The vector  $\mathbf{b}$  is, by design, continuous in the presence of medium discontinuities between horizontal layers, so we may proceed using the extrapolated  $\mathbf{b}$  as the boundary condition for the next layer.

Alternatively we may seek a more compact solution by premultiplying both sides of equation (1) by  $\mathbf{D}_{n+1}^{-1}$ , to obtain

$$\begin{aligned}\mathbf{v}(s_x, z_{n+1}+, \omega) &= \mathbf{W}(s_x; z_{n+1}+, z_{n+1}-) \mathbf{v}(s_x, z_{n+1}-, \omega) \\ &= \mathbf{W}(s_x; z_{n+1}+, z_{n+1}-) e^{i\omega \Lambda_n(z_{n+1}-z_n)} \mathbf{v}(s_x, z_n+, \omega),\end{aligned}\quad (2a)$$

$$\text{where } \mathbf{b}(s_x, z_n, \omega) = \mathbf{D}_n(s_x) \mathbf{v}(s_x, z_n+, \omega) = \mathbf{D}_{n-1}(s_x) \mathbf{v}(s_x, z_n-, \omega), \quad (2b)$$

$$\text{and } \mathbf{W}_{n+1}(s_x) = \mathbf{W}(s_x; z_{n+1}+, z_{n+1}-) = \mathbf{D}_{n+1}^{-1}(s_x) \mathbf{D}_n(s_x). \quad (2c)$$

As discussed in Bale and Margrave (2003), the three elements of  $\mathbf{v}$  are the amplitudes of P, S1 and S2 waves, which can be independently extrapolated in a homogeneous medium. Note that  $\mathbf{v}$ , unlike  $\mathbf{b}$ , is *not* necessarily continuous at  $z_n$ , which necessitates the use of the - and + qualifiers, to indicate just above and just below  $z_n$ , respectively. The 3-by-3 “interface-propagator” matrix  $\mathbf{W}$ , is simply the one-way transmission operator which determines the P, S1 and S2 amplitudes below  $z_n$ , from those above. Equation (2) requires approximately half the memory of equation (1), and initial results suggest it is approximately four times as CPU efficient, corresponding to the difference in operation count between applying two 3-by-6 matrix multiplies compared with a single 3-by-3 matrix multiply. Hence it is preferable, where possible, to formulate extrapolation in this form.

### PSPI and NSPS elastic extrapolation

We now consider PSPI and NSPS equivalents to equation (1), and the circumstances under which they may be transformed to the more efficient form of equation (2). The key modification is that  $\mathbf{D}_n$  and  $\Lambda_n$  now depend on *both*  $s_x$  and  $x$ .

The PSPI form of equation (1) is

$$\mathbf{b}_{PSPI}(x, z_{n+1}, \omega) = \frac{\omega}{2\pi} \int_{-\infty}^{\infty} \mathbf{D}_n(x, s_x) \mathbf{E}_n(x, s_x, \omega) \mathbf{D}_n^{-1}(x, s_x) \mathbf{b}(s_x, z_n, \omega) e^{-i\omega s_x x} ds_x, \quad (3)$$

$$\text{where } \mathbf{b}(s_x, z_n, \omega) = \int_{-\infty}^{\infty} \mathbf{b}(x, z_n, \omega) e^{i\omega s_x x} dx,$$

$$\mathbf{E}_n(x, s_x, \omega) = e^{i\omega \Lambda_n(x, s_x)(z_{n+1}-z_n)}, \quad (4)$$

$$\text{and } \Lambda_n(x, s_x) = \text{diag}(q_n^P(x, s_x) \quad q_n^{S1}(x, s_x) \quad q_n^{S2}(x, s_x)).$$

Similarly we may define the NSPS form of the elastic extrapolator as follows

$$\mathbf{b}_{NSPS}(s_x, z_{n+1}, \omega) = \int_{-\infty}^{\infty} \mathbf{D}_n(x, s_x) \mathbf{E}_n(x, s_x, \omega) \mathbf{D}_n^{-1}(x, s_x) \mathbf{b}(x, z_n, \omega) e^{i\omega s_x x} dx. \quad (5)$$

Equation (3) and (5) are similar to inverse and forward Fourier transforms, but since the kernel depends on both  $x$  and  $s_x$ , they are not standard Fourier transforms, but are instead pseudodifferential or Fourier integral operators, which cannot be directly implemented using FFT code.

The practical implementation of equations (3) or (5) is a complex issue. The standard PSPI approach is to first find the range of velocity variation and to design operators for each of a number of reference velocities within that range, then to apply spatially invariant operators for each reference velocity, and finally to interpolate the results based upon the spatially varying velocity. Unfortunately, while this is very effective for an acoustic extrapolation with only a single velocity parameter, we are here dealing with an operator which depends upon several parameters. The minimum number required to represent an HTI medium is six, which can be defined (among various equivalent ways) as:  $\alpha_0, \beta_0$ , the P- and S-wave velocities for propagation along the symmetry axis;  $\varepsilon, \delta, \gamma$ , the Thomsen parameters; and  $\phi$ , the orientation of the axis of symmetry within the horizontal plane. If we assume that only 5 reference values are selected for each parameter, then the total number of reference operators which would be computed is  $5^6 = 15625$ , which is clearly intractable. Another approach is to apply regular spatial windows for the operators, using either the parameter set corresponding to the center of the window, or some kind of window average. Assuming reasonably smooth variation of the medium, this appears a more economical approach, certainly for 2-D (or any narrow azimuth) cases. This is the approach used in this paper. Other possibilities include an adaptive windowing approach, such as adaptive Gabor phase-shift (AGPS) (Grossman et al., 2002a, 2002b), or some kind of hybrid scheme. For example, in a model where there are two main units, each with smooth internal variation but abrupt change across the boundary (e.g. entering a fracture zone), it might be appropriate to keep the anisotropy parameters fixed within each unit, and use a standard PSPI approach to vary the velocities internally to the units, or an alternative method such as split-step (Stoffa et al., 1990).

Following Ferguson and Margrave (1999), we reformulate (3) and (5) in terms of windows to obtain

$$\mathbf{b}_{PSPI}(x, z_{n+1}, \omega) = \frac{\omega}{2\pi} \sum_j \Omega_j(x - x_j) \int_{-\infty}^{\infty} \mathbf{P}_n(x_j, s_x, \omega) \mathbf{b}(s_x, z_n, \omega) e^{-i\omega s_x x} ds_x, \quad (6)$$

and

$$\mathbf{b}_{NSPS}(s_x, z_{n+1}, \omega) = \sum_j \mathbf{P}_n(x_j, s_x, \omega) \int_{-\infty}^{\infty} \Omega_j(x - x_j) \mathbf{b}(x, z_n, \omega) e^{i\omega s_x x} dx, \quad (7)$$

$$\text{where} \quad \mathbf{P}_n(x, s_x, \omega) = \mathbf{D}_n(x, s_x) \mathbf{E}_n(x, s_x, \omega) \mathbf{D}_n^{-1}(x, s_x). \quad (8)$$

Equations (6) and (7) arise from (3) and (5) when we approximate  $\mathbf{P}_n(x, s_x, \omega)$  by the sum of windowed locally constant functions

$$\mathbf{P}_n(x, s_x, \omega) \cong \sum_j \Omega_j(x - x_j) \mathbf{P}_n(x_j, s_x, \omega). \quad (9)$$

The window functions  $\Omega_j$  can be piecewise constant as in Ferguson and Margrave (1999), or linear (triangular), or a smoother function such as a Gaussian. An important characteristic of these windows is that they must form a partition of unity

$$\sum_j \Omega_j(x - x_j) = 1, \forall x. \quad (10)$$

Piecewise constant and linear windows can be constructed to satisfy (9). Gaussians do not strictly satisfy (9), but can be modified by normalization to do so (as can any set of well-behaved windows which cover the domain of  $x$ ). Partitions of unity are further discussed in Grossman et al. (2002b) and Bale et al. (2002).

### **Interface-propagator method**

For laterally homogeneous media, equation (2) describes an efficient extrapolation using 3-by-3 interface-propagator matrices. We now consider whether such an approach is viable for laterally heterogeneous extrapolation using pseudodifferential (PSPI/NSPS) type operators.

First, we write the extrapolation of the wave-mode vector,  $\mathbf{v}$ , using two pseudodifferential equations, one of an NSPS type, and the second of a PSPI type. This can obviously be done in more than one way, arriving at different but similar results. We use the following

$$\begin{aligned} \mathbf{b}(s_x, z_{n+1}, \omega) &= \int_{-\infty}^{\infty} \mathbf{D}_n(x', s_x) \mathbf{v}(x', z_{n+1}^-, \omega) e^{i\omega s_x x'} dx' \\ &= \int_{-\infty}^{\infty} \mathbf{D}_n(x', s_x) \mathbf{E}_n(x', s_x, \omega) \mathbf{v}(x', z_n^+, \omega) e^{i\omega s_x x'} dx', \end{aligned} \quad (11)$$

$$\text{and} \quad \mathbf{v}(x, z_{n+1}^+, \omega) = \frac{\omega}{2\pi} \int_{-\infty}^{\infty} \mathbf{D}_n^{-1}(x, s_x) \mathbf{b}(s_x, z_{n+1}, \omega) e^{-i\omega s_x x} ds_x. \quad (12)$$

Substitution of equation (11) into (12) gives

$$\begin{aligned} \mathbf{v}(x, z_n+, \omega) &= \frac{\omega}{2\pi} \int_{-\infty}^{\infty} \mathbf{D}_n^{-1}(x, s_x) \left\{ \int_{-\infty}^{\infty} \mathbf{D}_{n-1}(x', s_x) \mathbf{v}(x', z_n-, \omega) e^{i\omega s_x x'} dx' \right\} e^{-i\omega s_x x} ds_x \\ &= \frac{\omega}{2\pi} \int_{-\infty}^{\infty} \mathbf{W}_n(x, x', \omega) \mathbf{v}(x', z_n-, \omega) dx', \end{aligned} \quad (13a)$$

$$\text{where} \quad \mathbf{W}_n(x, x', \omega) = \int_{-\infty}^{\infty} \mathbf{D}_n^{-1}(x, s_x) \mathbf{D}_{n-1}(x', s_x) e^{i\omega s_x (x'-x)} ds_x. \quad (13b)$$

Since application of equation (13) entails a 3-by-3 matrix operation for each input point,  $x'$ , and each output point,  $x$ , it will be considerably less efficient than the homogeneous version of equation (2).

As before, we now introduce windowed versions of the spatially varying filters in the hopes of deriving a more efficient interface-propagator for heterogeneous media. Equation (11) becomes

$$\begin{aligned} \mathbf{b}(s_x, z_{n+1}, \omega) &= \sum_j \mathbf{D}_n(x_j, s_x) \mathbf{E}_n(x_j, s_x, \omega) \\ &\quad \int_{-\infty}^{\infty} \Omega_j(x' - x_j) \mathbf{v}(x', z_n+, \omega) e^{i\omega s_x x'} dx', \end{aligned} \quad (14)$$

while equation (12) becomes

$$\mathbf{v}(x, z_{n+1}+, \omega) = \frac{\omega}{2\pi} \sum_k \Omega_k(x - x_k) \int_{-\infty}^{\infty} \mathbf{D}_n^{-1}(x_k, s_x) \mathbf{b}(s_x, z_{n+1}, \omega) e^{-i\omega s_x x} ds_x. \quad (15)$$

Substituting (14) into (15), and interchanging the order of integrations, gives

$$\begin{aligned} \mathbf{v}(x, z_{n+1}+, \omega) &= \frac{\omega}{2\pi} \sum_k \Omega_k(x - x_k) \\ &\quad \sum_j \int_{-\infty}^{\infty} \mathbf{Y}_n^{(jk)}(x' - x, \omega) \Omega_j(x' - x_k) \mathbf{v}(x', z_n+, \omega) dx', \end{aligned} \quad (16)$$

where

$$\mathbf{Y}_n^{(jk)}(y, \omega) = \int_{-\infty}^{\infty} \mathbf{D}_n^{-1}(x_k, s_x) \mathbf{D}_n(x_j, s_x) \mathbf{E}_n(x_j, s_x, \omega) e^{i\omega s_x y} ds_x. \quad (17)$$

Application of equation (16) entails the following steps:

1. For each  $j$ , apply windowing function to  $\mathbf{v}$ .

2. For each  $j$  and  $k$ , apply (matrix) convolution of windowed  $\mathbf{v}$  by  $\mathbf{Y}_n^{(jk)}$ , summing over  $j$ .
3. For each  $k$  apply windowing function to result of 2, and sum over  $k$ .

Step 2 unfortunately makes this approach inefficient, compared with the more direct approach of equations (6) or (7), as it requires computation of the matrix convolution for all input and output window combinations. So, unlike the homogeneous case (which can be thought of as one input window, one output window), the advantage of using a 3-by-3 interface-propagator matrix for extrapolation are outweighed by the additional cost of using interface-propagators for all window pairs. We have not implemented equation (17) due to this undesirable cost.

Is this a general conclusion, or an artifact of the choice of where NSPS and PSPI approximations have been introduced? We consider as an alternative direct approximation of equation (2a) by a PSPI operator, as follows

$$\mathbf{v}(x, z_{n+1}+, \omega) = \frac{\omega}{2\pi} \int_{-\infty}^{\infty} \mathbf{W}_{n+1}(x, s_x) \mathbf{E}_{n+1}(x, s_x, \omega) \mathbf{v}(s_x, z_n+, \omega) e^{i\omega s_x x} ds_x, \quad (18)$$

where

$$\mathbf{W}_{n+1}(x, s_x) = \mathbf{W}(x, s_x; z_{n+1}+, z_{n+1}-) = \mathbf{D}_{n+1}^{-1}(x, s_x) \mathbf{D}_n(x, s_x). \quad (19)$$

In a windowed form this becomes:

$$\begin{aligned} \mathbf{v}_{PSPI}(x, z_{n+1}+, \omega) &= \frac{\omega}{2\pi} \sum_j \Omega_j(x - x_j) \\ &\int_{-\infty}^{\infty} \mathbf{W}_{n+1}(x_j, s_x) \mathbf{E}_{n+1}(x_j, s_x, \omega) \mathbf{v}(s_x, z_n+, \omega) e^{i\omega s_x x} ds_x. \end{aligned} \quad (20)$$

Equation (20) describes a relatively efficient algorithm, which consists of applying both phase shift operators and interface-propagators for each window, in the spatial slowness domain, applying inverse Fourier transforms and then summing the spatially windowed results. Because the matrices involved are 3-by-3, equation 20 has the same cost advantage as equation (2) when compared to equation (6). Another advantage with equation (20) is that the terms in  $\mathbf{W}$  are can be selected to discriminate against some modes, such as P-S conversion. However, comparison of numerical results from using equation (20) with those using equation (6) suggest that it gives a worse approximation when the assumption of smooth model variation is violated. With the help of Figure 1, we offer an explanation of this observation.

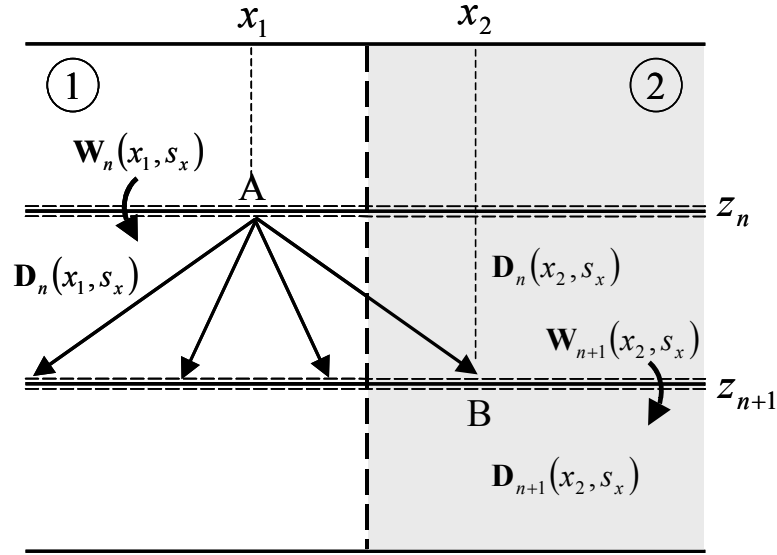


FIG. 1. Extrapolation across a lateral discontinuity. Medium 1 (white) and medium 2 (shaded) are homogeneous with different anisotropic symmetry axes.

First of all it is important to reiterate that PSPI and NSPS are approximations to the exact solution. The nature of the approximation can be understood by considering extrapolation as generation of Huygens wavefronts using locally constant parameters (Margrave and Ferguson, 1998): velocity for acoustic case, anisotropic stiffnesses for the elastic case. The parameters of the wavefield extrapolator are either those of the output position (PSPI) or of the input position (NSPS), rather than those which characterize the path between the two. The error in this approximation becomes smaller as the depth step becomes smaller, but in the presence of discontinuous lateral changes it never disappears. In the case of acoustic extrapolation the result is a phase error, but in the elastic case a more serious error can occur if we are not careful, due to polarization. Consider the extrapolation of data from point A to point B in Figure 1, across the boundary between medium 1, and medium 2. Assume also that there is a change in the polarization of the shear waves associated with the boundary. If PSPI extrapolation is performed using equation (6), then the decomposition and recomposition matrices used are  $\mathbf{D}_n^{-1}(x_2, s_x)$  and  $\mathbf{D}_n(x_2, s_x)$ , corresponding to the output point B, with lateral position  $x_2$ . These are *self-consistent*, in the sense that the polarization of the P, S1 and S2 modes are taken to be the same at A and B. Similarly NSPS extrapolation using equation (7) uses decomposition and recomposition matrices defined at the input point with lateral position  $x_1$ . While they clearly will give results different from equation (6), they are once again self-consistent. Now, consider using equation (20). At point A, the interface propagator used is  $\mathbf{W}_n(x_1, s_x)$ , which implies decomposition based on medium 1 parameters. At point B, the interface propagator used is  $\mathbf{W}_{n+1}(x_2, s_x)$ , which implies recomposition based on medium 2 parameters. These are *self-inconsistent* operators. For example, suppose the orientation of the axis of symmetry differs between the two media by  $90^\circ$ . The polarization of S1 in medium 1, becomes approximately the polarization of S2 in medium 2. The result of using equation (20) is an unwanted flipping of modes, as

energy which started at point A with one polarization is interpreted at point B to have a completely different polarization. It is in fact the need for self-consistency which gives rise to the (expensive) interaction between windows in equation (17).

The errors resulting from extrapolation across a discontinuity with equation (20) are illustrated in the following section in Figure 5. However, as shown in Figure 6, the errors are small in the presence of *continuous* changes in polarization. Hence, we could choose to use the less accurate, but more efficient equation (20) provided the changes in anisotropy axis are gradual.

## RESULTS

We now illustrate the use of the above extrapolation operators with numerical results.

### PSPI and NSPS elastic extrapolation tests

Figure 2 illustrates the result of extrapolating three impulses by 400m downwards in a single step, for an HTI medium with an abrupt change in symmetry direction in the center. Two homogeneous extrapolations are shown for reference. In (a) the extrapolation is for a homogeneous medium with a symmetry axis in the x-direction. In (b) the extrapolation is for a homogeneous medium with symmetry axis at  $45^\circ$  to the x-direction. In (c) and (d) the medium is the same as in (a) for the left half, and the same as in (b) for the right half. In (c) we have extrapolated using the windowed PSPI algorithm of equation (6), with a fixed window size of 80m (8 times trace spacing) and using linearly tapered windows. For PSPI the windowing is applied to the output, which is clearly visible in the abrupt onset of S1 energy in the center of the section. In (d) we have used the NSPS algorithm of equation (7) with the same window parameters as in (c). Since the windowing is applied on input for NSPS, we now see that 2 of the 3 impulses contribute to the S1 energy (the second impulse lies on the boundary, which explains the lower S1 amplitude associated with it). Figure 3 shows the reverse extrapolation of the PSPI and NSPS results in Figure 2. The ideal result would be three bandlimited spikes only present on the vertical (Z) component. Note that, as was found to be the case for scalar extrapolation, the NSPS operator appears to invert the PSPI result and vice versa. This suggests that for the (vector) elastic case, as has been proven in the (scalar) acoustic case by Margrave and Ferguson (1998), NSPS and PSPI are adjoint operators when used in opposite directions.

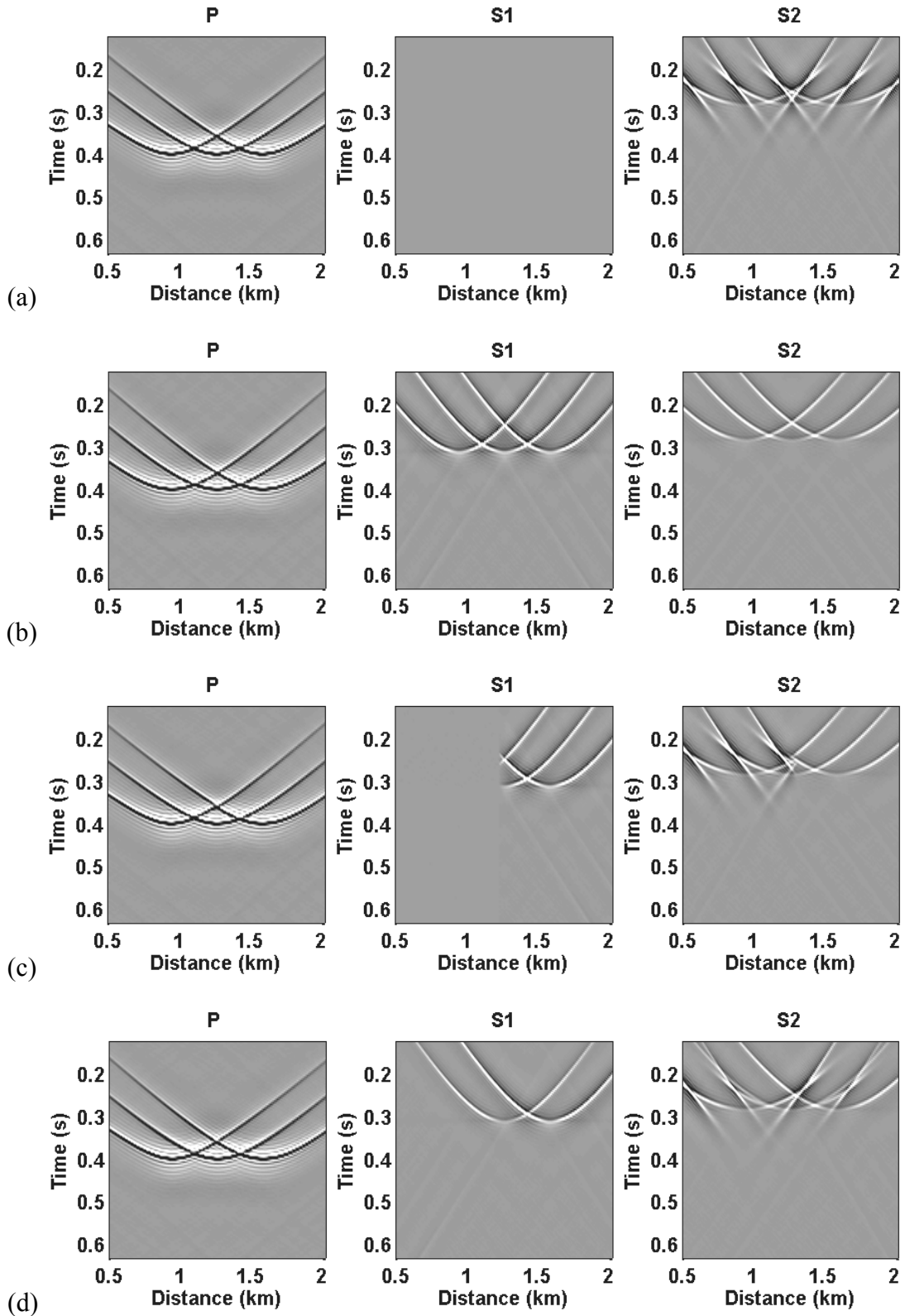


FIG. 2. Example of elastic PSPI and NSPS extrapolation in a single step for a medium with a discontinuous change of anisotropic symmetry direction. (a) Homogeneous model with  $0^\circ$  symmetry axis; (b) homogeneous model with  $45^\circ$  symmetry axis; (c) PSPI using linearly tapered windows spaced at 80m; (d) NSPS using same windows for discontinuous model.

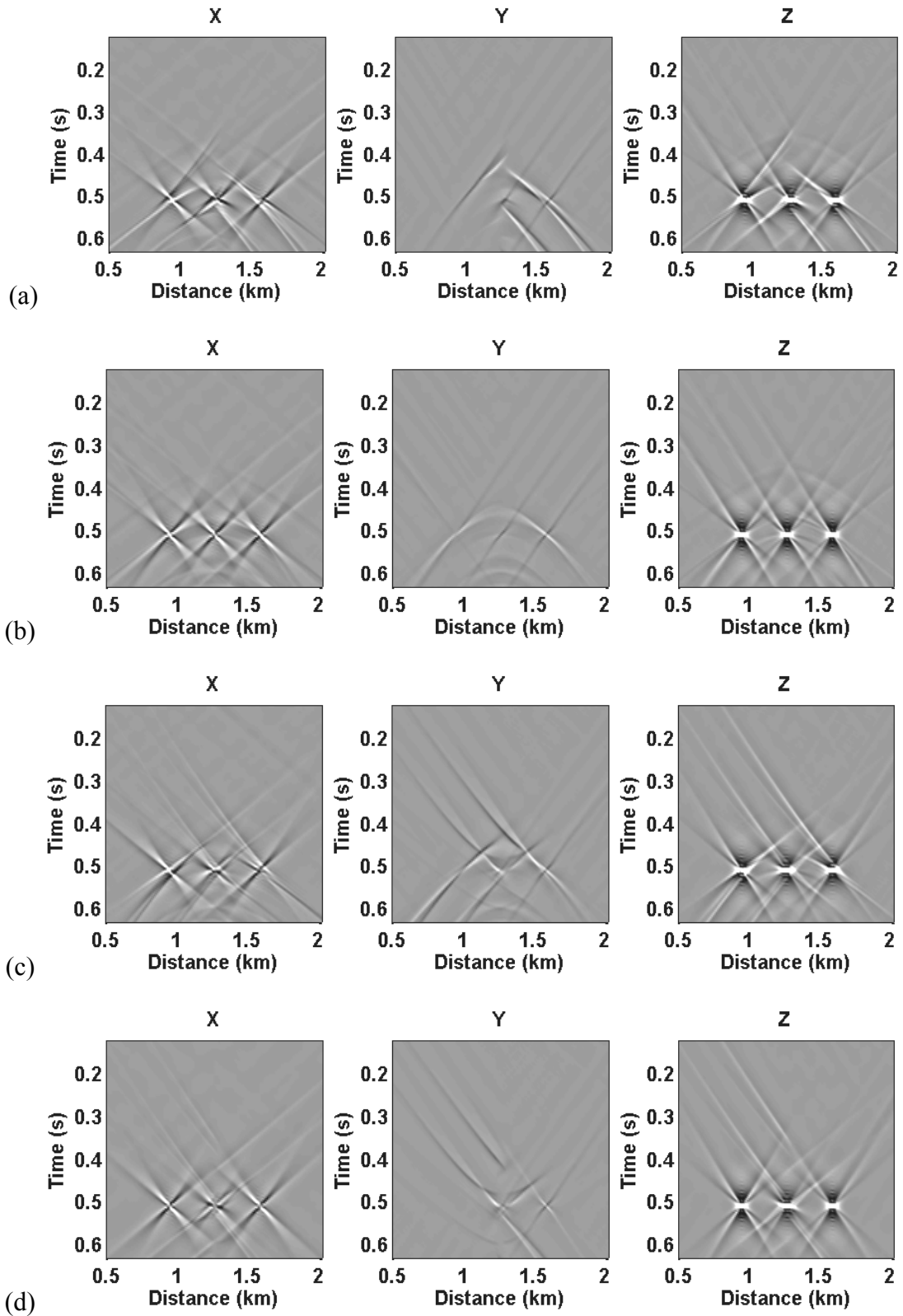


FIG. 3. Inverse extrapolation (a) PSPI forward and reverse; (b) PSPI forward, NSPS reverse; (c) NSPS forward and reverse; (d) NSPS forward, PSPI reverse.

## Comparison with interface-propagator method

Figure 4 shows two models used to test the interface-propagator approximation in equation (20), one with a discontinuous  $90^\circ$  change of symmetry axis, and the other with a linear change of symmetry axis over several windows.

For the discontinuous jump (4a) the physics of anisotropic wave-propagation dictate that *no energy should be generated on the Y-component*, since the x-z plane is a plane of symmetry for both left and right halves of the model. In Figure 5, we compare the PSPI extrapolation using equation (6) ((a) and (b)) with the result of equation (20) ((c) and (d)). In both cases linearly tapered windows of 40m (4 times trace interval) are used. The wave-mode amplitudes are shown in (a) and (c). The corresponding displacements are shown in (b) and (d). In (b) the Y-component amplitude remains zero as it should, whereas in (d) we observe (incorrect) assignment of energy onto the Y-component. We see that in this case, equation (20) gives significantly erroneous results in polarization, which are not present for equation (6). Of course, it is still true for equation (6) that there are errors of phase due to the PSPI approximation.

Our last example, in Figure 6, considers the above comparison for the continuously varying symmetry axis direction of Figure 4(b). In contrast to the abrupt change of symmetry direction in the previous example, it is no longer correct to expect absence of energy on the Y-component, as the transition includes symmetry directions in all azimuths between  $0^\circ$  and  $90^\circ$ , which certainly generate rotated polarizations. Furthermore there is now very good agreement between the results using equation (6) and those using equation (20) (compare (b) and (d)), as anticipated. This supports the assertion that equation (20) may still be appropriate for cases where there are expected to be smooth changes in anisotropy.

## CONCLUSIONS

The PSPI and NSPS methods have been used to extend our elastic wavefield extrapolation algorithm to media with lateral variations, including changes in the HTI symmetry axis. This can be done in more than one way, with a choice not only of PSPI vs. NSPS, but whether to use full extrapolation of the displacement-stress wavefield, or the more compact extrapolation of wave-modes using interface-propagators. The interface-propagators, if posed in a form which retains the efficiency advantage, have associated errors in the presence of rapid changes of symmetry axis. Generally, we therefore advocate the use of the full displacement-stress extrapolation. Nevertheless, if the medium can be assumed to have slowly varying changes of symmetry axis, then numerical results suggest the more efficient interface-propagator method is appropriate.

## ACKNOWLEDGEMENTS

The authors would like to acknowledge the support of sponsors of the CREWES project and of the POTSI project, towards this work. The authors also thank Jeff Grossman and Hugh Geiger for stimulating discussions on this topic.

## REFERENCES

- Bale, R.A., Grossman, J.P., Margrave, G.F., and Lamoureux, M.P., 2002, Multidimensional partitions of unity and Gaussian terrain: CREWES Research Report, **14**.
- Bale, R.A. and Margrave, G.F., 2003, Elastic wavefield extrapolation in HTI media: CREWES Research Report, Vol. **15**, this volume.
- Ferguson, R.J. and Margrave, G.F., 2002, Prestack depth migration by symmetric nonstationary phase shift: *Geophysics*, **67**, 594-603.
- Gazdag, J. and Sguazero, P., 1984, Migration of seismic data by phase shift plus interpolation: *Geophysics*, **49**, 124 - 131.
- Grossman, J.P., Margrave, G.F., and Lamoureux, M.P., 2002a, Fast wavefield extrapolation by phase-shift in the nonuniform Gabor domain: CREWES Research Report, **14**.
- Grossman, J.P., Margrave, G.F., and Lamoureux, M.P., 2002b, Constructing adaptive nonuniform Gabor frames from partitions of unity: CREWES Research Report, **14**.
- Margrave, G.F. and Ferguson, R.J., 1998, Explicit Fourier wavefield extrapolators: CREWES Research Report, Vol. **10**.
- Margrave, G.F. and Ferguson, R.J., 1999, Wavefield extrapolation by nonstationary phase shift: *Geophysics*, **64**, 1067-1078.
- Margrave, G. and Ferguson, R., 2000, Taylor series derivation of nonstationary wavefield extrapolators: 70th Ann. Internat. Mtg: Soc. of Expl. Geophys., 834-837.
- Stoffa, P.L., Fokkema, J.T., de Luna Freire, R.M., and Kessinger, W.P., 1990, Split-step Fourier migration: *Geophysics*, **55**, 410-421.
- Ting, T.C.T., 1996, *Anisotropic Elasticity: Theory and Applications*: Oxford University Press.

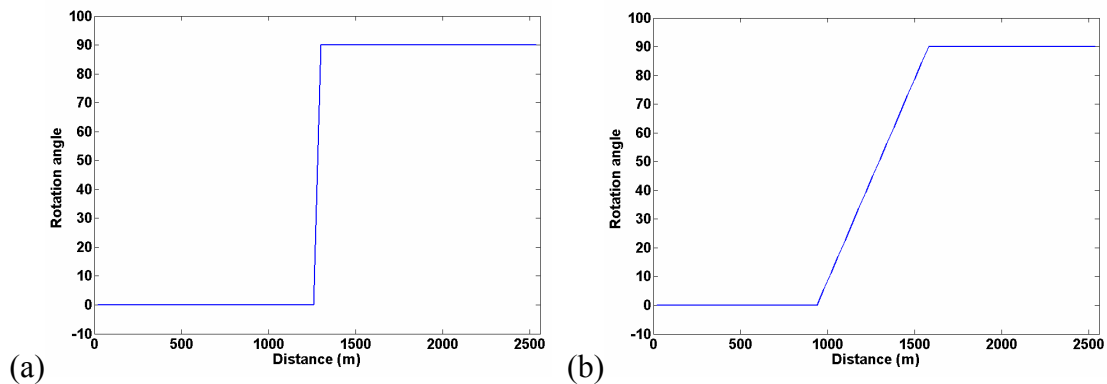


FIG. 4. Rotation angle variation along 2-D line; (a) discontinuous jump; (b) gradient.

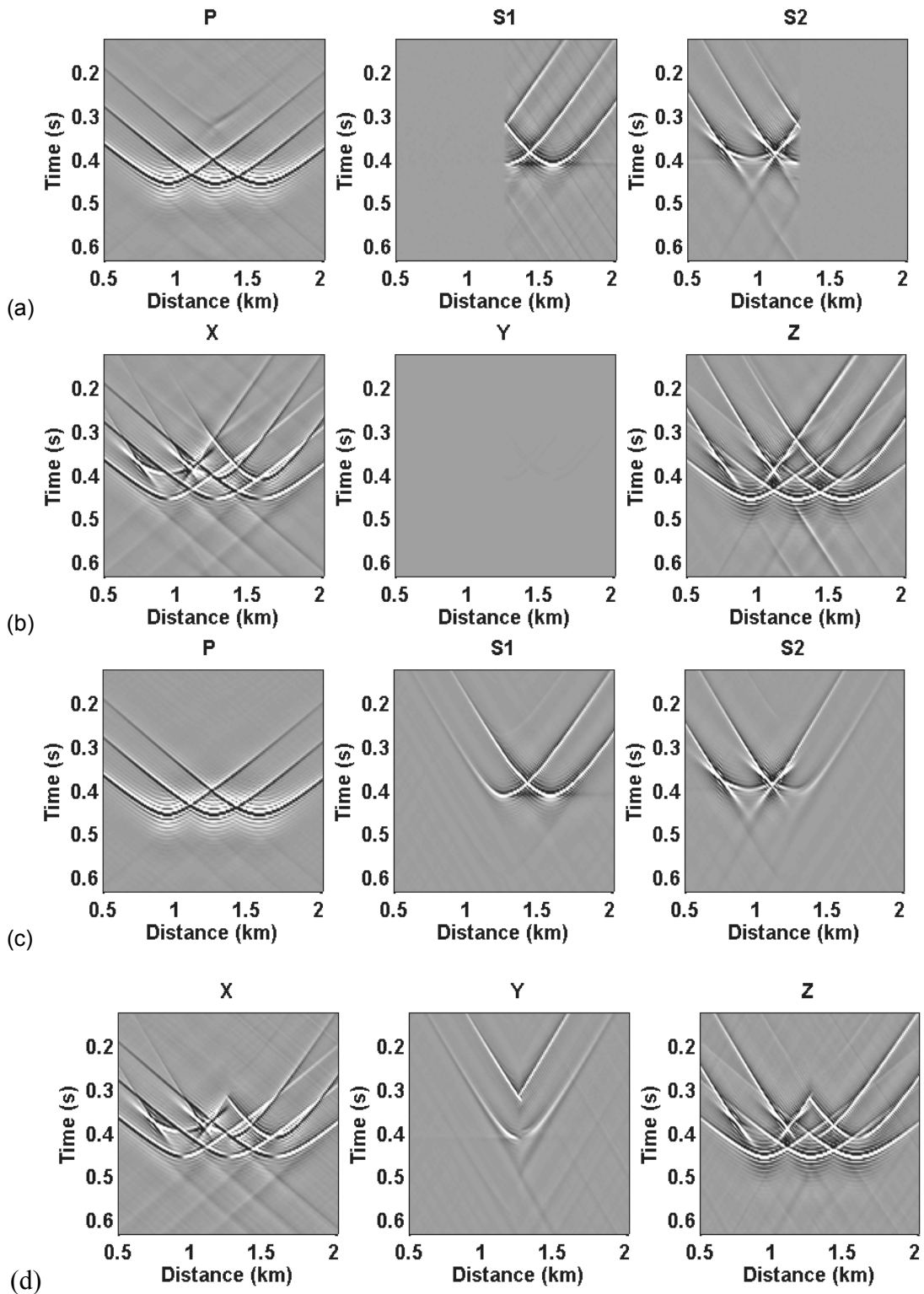


FIG. 5. PSPI with 40m window spacing for abrupt change of anisotropic symmetry direction. (a) Extrapolation using full displacement-stress representation at interfaces; (b) displacements corresponding to (a); (c) extrapolation using interface-propagators; (d) displacements corresponding to (c).

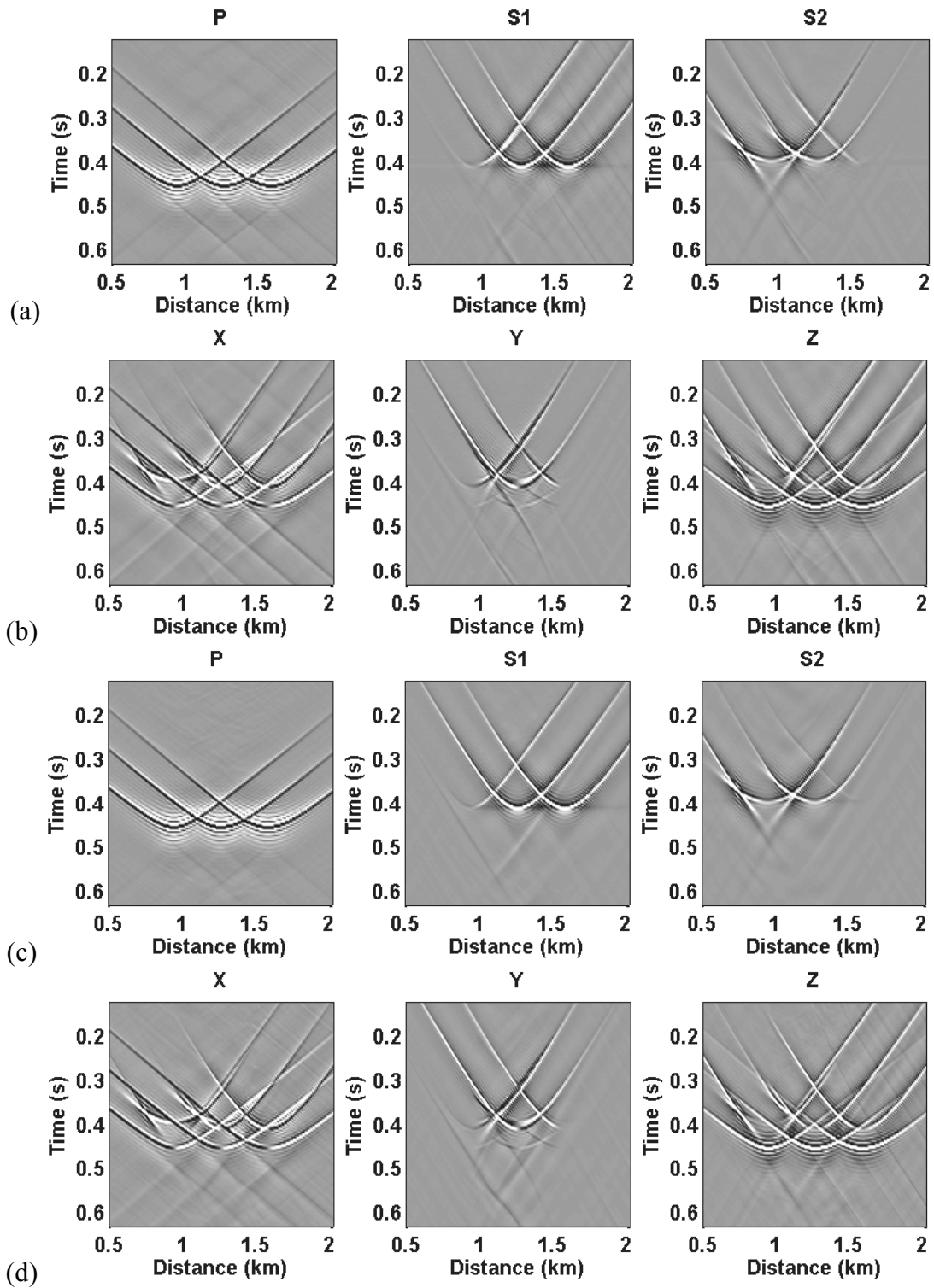


FIG. 6. PSPI with 40m window spacing for gradual change of anisotropic symmetry direction. (a) Extrapolation using full displacement-stress representation at interfaces; (b) displacements corresponding to (a); (c) extrapolation using interface-propagators; (d) displacements corresponding to (c).